SAND2011-2457C

Clutter locus equation for more general linear array orientation

Douglas L. Bickel
Sandia National Laboratories, 1515 Eubank Blvd. SE, Albuquerque, NM, USA 87185-0519

ABSTRACT

The clutter locus is an important concept in space-time adaptive processing (STAP) for ground moving target indicator (GMTI) radar systems. The clutter locus defines the expected ground clutter location in the angle-Doppler domain. Typically in literature, the clutter locus is presented as a line, or even a set of ellipsoids, under certain assumptions about the geometry of the array. Most often, the array is assumed to be in the horizontal plane containing the velocity vector. This paper will give a more general 3-dimensional interpretation of the clutter locus for a general linear array orientation.

Keywords: Clutter locus, space-time adaptive processing, array orientation

1. INTRODUCTION

The clutter locus in space-time adaptive processing (STAP) represents the stationary ground clutter location in the angle-Doppler domain. STAP seeks to filter the interference from stationary clutter along this clutter locus while maximizing the return from the desired moving object. The geometry of the clutter locus is set by the array orientation relative to the platform velocity vector. This paper brings together in a single 3-dimensional equation various clutter locus models presented in literature for the general orientation of a uniform linear array.

2. CLUTTER LOCUS

The clutter locus equation for general orientation of a linear array is presented in this section. This discussion will expand on the equations and plots given in section 3.1 of [1]. As in this portion of the reference, we will assume that the array and Doppler are adequately sampled. We will also ignore other clutter effect such as internal motion, jammers, etc. This section will emphasize the 3-dimensional nature of the clutter locus equation and show how this equation brings together other concepts on the clutter locus presented in literature.

2.1 Clutter locus

The standard presentation of the clutter locus is given in [1]. Figure 1 illustrates the standard clutter locus curves as shown in [1]. Figures 1a-1d show the clutter locus curves for four different rotations of the array with respect to the velocity vector. Both the array and the velocity vector are in the horizontal plane. The different colors within each of the subplots represent the clutter loci for different ground grazing angles.

2.2 3-D Clutter locus

A general equation for the clutter locus is derived in Appendix A:

$$A\zeta_1^2 + B\zeta_0^2 + C\zeta_0\zeta_1 + D_1\zeta_1 + D_2\zeta_1\zeta_\Psi + E_1\zeta_0 + E_2\zeta_0\zeta_\Psi + F_1 + F_2\zeta_\Psi^2 + G\zeta_\Psi = 0 \qquad (1)$$

Equation (1) can be recognized as a quadric equation in 3-dimensions. In particular, for the bounds that naturally fall out of the coefficients in this equation, it can be shown to geometrically represent a triaxial, or scalene, ellipsoid. Typically the clutter locus presented in literature just show 2-dimensional samplings of the 3-dimesional equation and often do not point out the 3-dimensional nature of the clutter locus. The author in [2] and a few others do point out the 3-dimensional nature of the clutter locus curves, but do not present the general case, or give a general equation.

Figure 2 shows a 3-dimensional example of the ellipsoid from equation (1). Figure 3 repeats Figure 2, with the exception that grazing angles above the horizon are ignored for ground imaging applications.

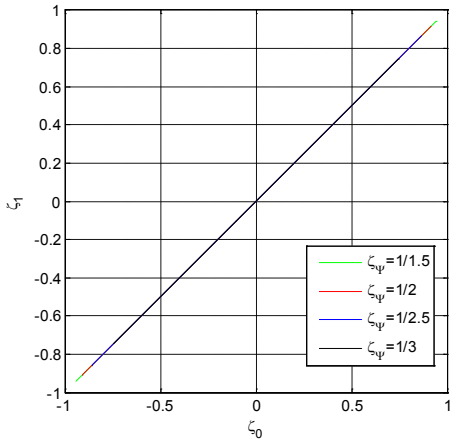

(a) 0° array rotation in horizontal plane

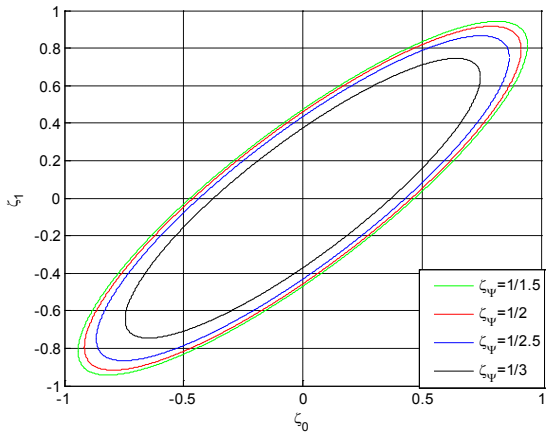

(b) 30° array rotation in horizontal plane

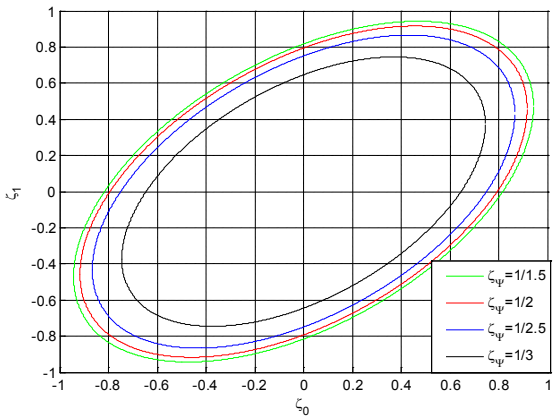

(c) 60° array rotation in horizontal plane

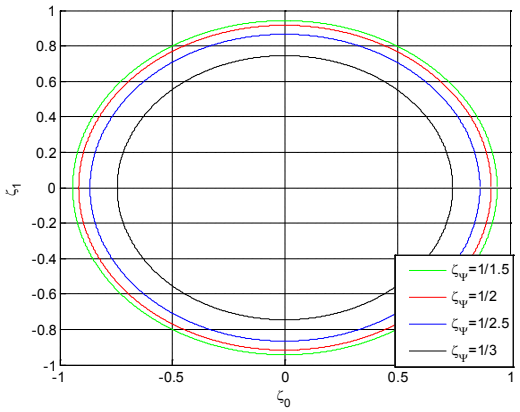

(d) 90° array rotation in horizontal plane

Figure 1: Clutter locus curves for grazing angles and various horizontal array orientations (a la [1])

2.3 Limiting cases of the clutter locus equation

Figure 1b can be readily observed to be equivalent to specific slices through the ellipsoid from Figure 3 (or Figure 2) evaluated for different values of the ζ_Ψ. In general, all of the subplots in Figure 1 can be shown to be limiting cases of equation (1) where the array and the velocity vector are in the horizontal plane. From the notation in the Appendix A, this case corresponds to $\gamma = 1$ and $\eta = 0$ with variations in κ. For this case, equation (1) becomes:

$$\frac{\zeta_1^2}{\left(1-\kappa^2\right)\left(1-\zeta_\Psi^2\right)} + \frac{\zeta_0^2}{\left(1-\kappa^2\right)\left(1-\zeta_\Psi^2\right)} - \frac{2\kappa\zeta_0\zeta_1}{\left(1-\kappa^2\right)\left(1-\zeta_\Psi^2\right)} = 1 \tag{2}$$

Equation (2) is the equation for an ellipse where the semiaxes are rotated by 45° in the $\zeta_0 - \zeta_1$ plane, and the semiaxes after rotation are $\sqrt{\left(1+\kappa\right)\left(1-\zeta_\Psi^2\right)}$ and $\sqrt{\left(1-\kappa\right)\left(1-\zeta_\Psi^2\right)}$ respectively. Figure 1a is the clutter locus that occurs when the array and the velocity vector are aligned ($\kappa = 1$). Equation (2) becomes the equation of a straight line also rotated by 45° in the $\zeta_0 - \zeta_1$ plane, given by:

$$\zeta_0 = \zeta_1 \tag{3}$$

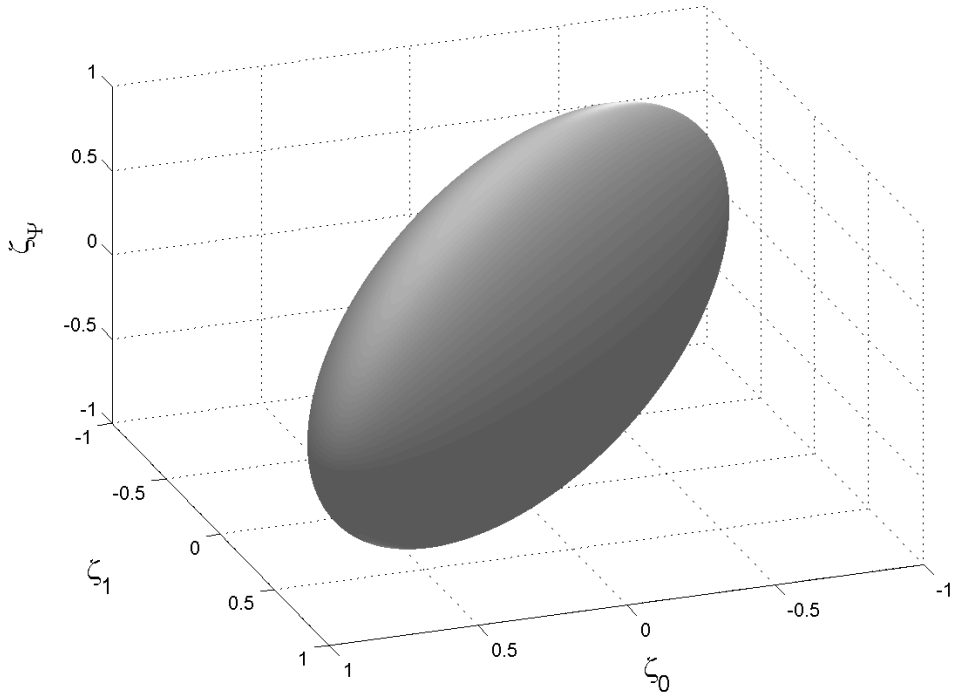

Figure 2: Clutter locus ellipsoid for level flight and level array rotated in the horizontal plane (30º "squint")

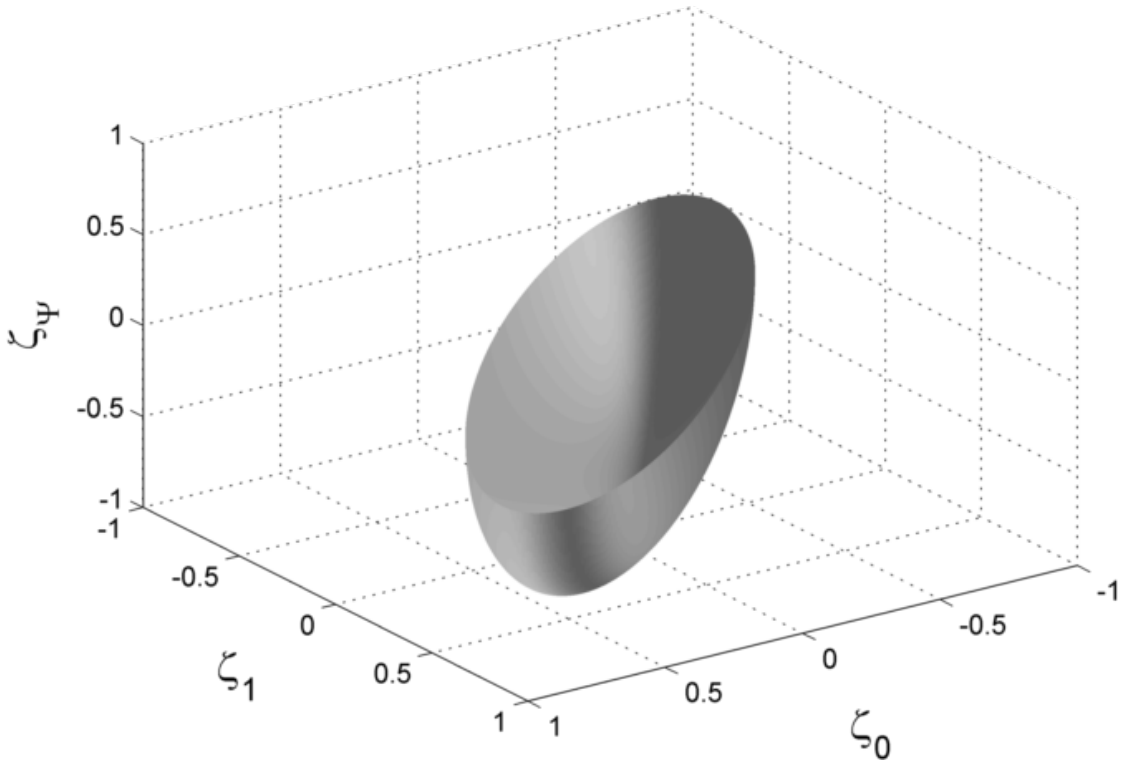

Figure 3: Equivalent to a Figure 2 with grazing angles above the horizon removed

2.4 Degenerate cases and 3-D perspective

Discussion of the rotations and semiaxes for the general case are presented in Appendix B. This section focuses on the 3-D perspective of the degenerate cases. The best example is equation (3) in the previous section. The equation appears to be that of a straight line; however, in 3-D it is really the result of the intersection of constant ζ_Ψ -planes with a degenerate ellipsoid case. In this case when $\kappa = 1$, one of the semiaxes (orthogonal to the $\zeta_0 = \zeta_1$ plane) degenerates to zero, and the other (along the $\zeta_0 = \zeta_1$ plane) becomes $\sqrt{2}\sqrt{\left(1-\zeta_\Psi^2\right)}$. Figure 4 shows the degenerate 3D ellipsoid below the horizon that leads to Figure 1a.

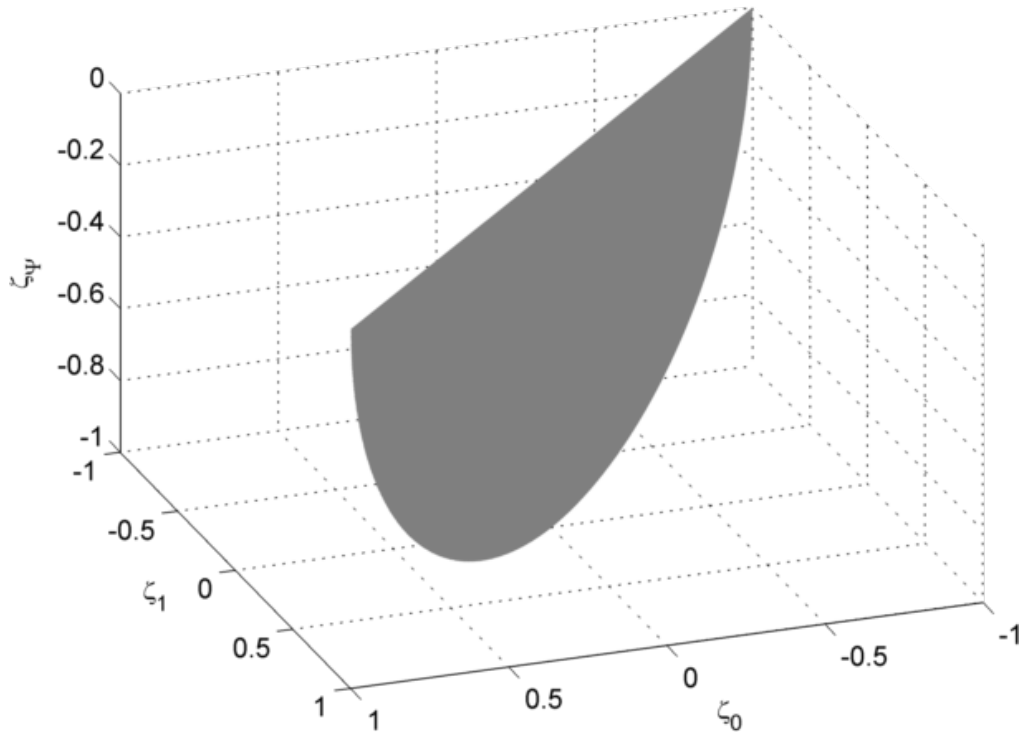

Figure 4: Degenerate 3D ellipsoid for array aligned with velocity vector

Another degenerate case of interest is the inclined array [3]. This case occurs, for example, when we are attempting to align the array with the velocity vector in the presence of aircraft pitch. The result is that the array is inclined vertically. For this case equation (1) becomes:

$$\zeta_1 = \sqrt{1-\eta^2}\,\zeta_0 + \eta\zeta_\Psi \tag{4}$$

For the traditional 2D viewpoint in the $\zeta_0 - \zeta_1$ plane, equation (4) is a sequence of lines whose offsets are a function of the grazing angle and whose slopes are no longer 45°. They are a function of the array inclination angle for $\eta \neq 0$. This result is rather intuitive. It says that the inclination of the array has two effects, corresponding to the two terms on the right-hand-side (rhs) of equation (4). The first term of the rhs is the result of foreshortening the array component in the direction of the velocity vector due to the array inclination. The second term of the rhs is the new sensitivity of the array to elevation angles due to the elevation component of the array. The latter is familiar to those who work with interferometric synthetic aperture radar for height measurement (see Chapter 5 of [4], for example). Figure 5 shows an example of the degenerate ellipsoid for 30° array inclination.

Other degenerate cases can be derived from equation (1), such as the forward-looking case [2], but are not presented in this paper. More details on the degenerate ellipsoids are presented in Appendix B.

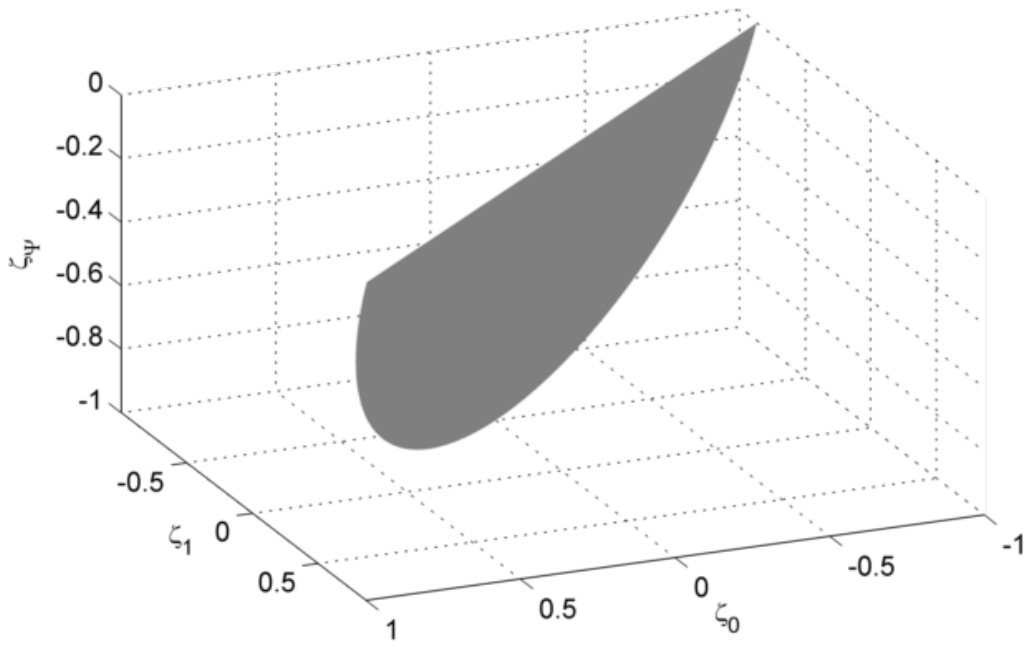

Figure 4: Degenerate 3D ellipsoid for array inclined by 30°

3. CONCLUSIONS

This paper presented a single equation for the clutter locus for general array orientation in space-time adaptive processing. This equation brings together the various clutter locus concepts presented in literature into a 3-dimensional perspective. This equation was shown to explain the standard 2-dimensional clutter locus plots typically found in literature [1], as well as other clutter locus equations, such as inclined arrays [3], and forward-looking arrays [2].

4. APPENDIX A: EQUATION DERIVATIONS

This appendix derives the general clutter locus equation for a uniform linear array.

Variable definitions

$\vec{u}_B$ - is the unit vector along the array

$\vec{u}_v$ - is the unit vector along the velocity

$\vec{u}_r$ - is the unit vector in the direction of the target

$\vec{u}_x$ - is the unit vector in the x-direction

$\vec{u}_y$ - is the unit vector in the *y*-direction

$\vec{u}_z$ - is the unit vector in the *z*-direction

ζ_0 - is the normalized Doppler defined by equation (5)

ζ_1 - is the normalized array response defined by equation (6)

κ - direction cosine between $\vec{u}_B$ and $\vec{u}_v$ (related to "squint" for a gimbaled antenna)

γ - direction cosine between $\vec{u}_v$ and $\vec{u}_x$

η - direction cosine between $\vec{u}_B$ into $\vec{u}_z$

$\zeta_\Psi = \vec{u}_z \cdot \vec{u}_r$ - the direction cosine between the range to the target and the *z*-axis

Additional geometry information

$\vec{u}_x$ and $\vec{u}_y$ are parallel to a horizontal ground plane. Choose $\vec{u}_x$ to be aligned with the projection of $\vec{u}_v$ into the horizontal plane, and $\vec{u}_y$ completes the right-hand-rule.

Base equations for derivation

$$\zeta_0 = \vec{u}_v \cdot \vec{u}_r \tag{5}$$
$$\zeta_1 = \vec{u}_B \cdot \vec{u}_r \tag{6}$$

where:
ζ_0, ζ_1 - are normalized quantities measured by the radar that are dependent upon the target direction

Derivation
Given the definitions and equations above, equation (5) can be rewritten as:

$$\zeta_0 = \gamma\left(\vec{u}_r \cdot \vec{u}_x\right) + \sqrt{1-\gamma^2}\zeta_\Psi \tag{7}$$

Rearranging, yields:

$$\vec{u}_r \cdot \vec{u}_x = \frac{\zeta_0 - \sqrt{1-\gamma^2}\zeta_\Psi}{\gamma} \tag{8}$$

By the definitions and with a little rearranging we get:

$$\vec{u}_B \cdot \vec{u}_x = \frac{\kappa - \eta\sqrt{1-\gamma^2}}{\gamma} \tag{9}$$

and:

$$\vec{u}_B \cdot \vec{u}_y = \frac{1}{\gamma}\sqrt{\gamma^2 - \left(\kappa^2 + \eta^2\right) + 2\kappa\eta\sqrt{1-\gamma^2}} \tag{10}$$

In a similar manner, using equation (6) along with equations (8) to (10) and rearranging, we can arrive at:

$$\vec{u}_r \cdot \vec{u}_y = \frac{1}{\gamma}\sqrt{\gamma^2 - \left(\zeta_0^2 + \zeta_1^2\right) + 2\zeta_0\zeta_1\sqrt{1-\gamma^2}} \tag{11}$$

Now equation (6) becomes:

$$\begin{aligned}\zeta_1 = {} & \frac{\left(\kappa - \eta\sqrt{1-\gamma^2}\right)\left(\zeta_0 - \sqrt{1-\gamma^2}\zeta_\Psi\right)}{\gamma^2} \\ & + \left(\sqrt{1 - \frac{\left(\kappa^2+\eta^2\right)}{\gamma^2} + \frac{2\kappa\eta\sqrt{1-\gamma^2}}{\gamma^2}}\right)\left(\sqrt{1 - \frac{\left(\zeta_0^2+\zeta_1^2\right)}{\gamma^2} + \frac{2\zeta_0\zeta_1\sqrt{1-\gamma^2}}{\gamma^2}}\right) + \eta\zeta_\Psi\end{aligned} \tag{12}$$

Finally, equation (12) can be re-organized to the form of equation (1)

$$A\zeta_1^2 + B\zeta_0^2 + C\zeta_0\zeta_1 + D_1\zeta_1 + D_2\zeta_1\zeta_\Psi + E_1\zeta_0 + E_2\zeta_0\zeta_\Psi + F_1 + F_2\zeta_\Psi^2 + G\zeta_\Psi = 0 \tag{1}$$

where the coefficients are:

$$A = \gamma^2$$
$$B = 1 - \eta^2$$

$$C = 2\left(\eta\sqrt{1-\gamma^2} - \kappa\right)$$
$$D_1 = 0$$
$$D_2 = 2\left(\kappa\sqrt{1-\gamma^2} - \eta\right)$$
$$E_1 = 0$$
$$E_2 = 2\left(\eta\kappa - \sqrt{1-\gamma^2}\right)$$
$$F_1 = -\gamma^2 + \eta^2 + \kappa^2 + 2\eta\kappa\sqrt{1-\gamma^2}$$
$$F_2 = \left(1-\kappa^2\right)$$
$$G = 0$$

5. APPENDIX B: ELLIPSOID PERSPECTIVE

This section discusses general properties that can be derived from the quadric form of the ellipsoid used in equation (1).

Properties of ellipsoid from quadric form

The quadric form of the 3-D ellipsoid equation can be written in matrix form. In the 3-D case we have:

$$x^T Q x + x^T q = 0 \tag{13}$$

where:

$$x^T = \begin{bmatrix} \zeta_0 & \zeta_1 & \zeta_\Psi & 1 \end{bmatrix}$$
$$Q = \begin{bmatrix} B & C/2 & E_2/2 & 0 \\ C/2 & A & D_2/2 & 0 \\ E_2/2 & D_2/2 & F_2 & 0 \\ 0 & 0 & 0 & F_1 \end{bmatrix}$$
$$q^T = \begin{bmatrix} E_1 & D_1 & G & 0 \end{bmatrix}$$

For simplicity in the discussion, in this section we will assume that the velocity vector is in the horizontal plane (i.e., $\gamma = 1$). If the velocity vector is not in the horizontal plane, there is an additional rotation that has to be accounted for in the discussion.

For $\gamma = 1$ the ellipsoid from equation (1) becomes:

$$\left(\frac{1}{1-\kappa^2-\eta^2}\right)\zeta_1^2 + \left(\frac{1-\eta^2}{1-\kappa^2-\eta^2}\right)\zeta_0^2 - \left(\frac{2\kappa}{1-\kappa^2-\eta^2}\right)\zeta_0\zeta_1 - \left(\frac{2\eta}{1-\kappa^2-\eta^2}\right)\zeta_1\zeta_\Psi + \left(\frac{2\eta\kappa}{1-\kappa^2-\eta^2}\right)\zeta_0\zeta_\Psi + \left(\frac{1-\kappa^2}{1-\kappa^2-\eta^2}\right)\zeta_\Psi^2 = 1 \tag{14}$$

The first property of this ellipsoid is that the origin is at $\left(\zeta_0, \zeta_1, \zeta_\Psi\right) = \left(0,0,0\right)$. This is a handy property, but note that this does not mean that the 2-D slices for a given ζ_Ψ value will necessarily be centered around $\left(\zeta_0, \zeta_1\right) = \left(0,0\right)$ for the general case.

The second property is that the rotation matrix to align the ellipsoid to the semiaxes is given by:

$$R = \begin{bmatrix} \frac{\kappa}{\sqrt{2}\sqrt{\kappa^2+\eta^2}} & -\frac{\kappa}{\sqrt{2}\sqrt{\kappa^2+\eta^2}} & -\frac{\eta}{\sqrt{\kappa^2+\eta^2}} & 0 \\ \frac{1}{\sqrt{2}} & \frac{1}{\sqrt{2}} & 0 & 0 \\ \frac{\eta}{\sqrt{2}\sqrt{\kappa^2+\eta^2}} & -\frac{\eta}{\sqrt{2}\sqrt{\kappa^2+\eta^2}} & -\frac{\kappa}{\sqrt{\kappa^2+\eta^2}} & 0 \\ 0 & 0 & 0 & -1 \end{bmatrix} \tag{15}$$

When the array and the velocity vector are contained in the horizontal plane, $\eta = 0$ equation (15) becomes:

$$R\big|_{\eta=0} = \begin{bmatrix} \frac{1}{\sqrt{2}} & -\frac{1}{\sqrt{2}} & 0 & 0 \\ \frac{1}{\sqrt{2}} & \frac{1}{\sqrt{2}} & 0 & 0 \\ 0 & 0 & 1 & 0 \\ 0 & 0 & 0 & 1 \end{bmatrix} \tag{16}$$

It is easy to recognize that the rotation for the horizontal plane case is 45° about the ζ_Ψ axis. This rotation of 45° is the value presented in literature. It is also readily observed in Figure 1.

Note that we can get equation (15) as the concantenation of rotation matrices using equation (16):

$$R = R_T R\big|_{\eta=0} \tag{17}$$

where:

$$R_T = \begin{bmatrix} \frac{\kappa}{\sqrt{\kappa^2+\eta^2}} & 0 & -\frac{\eta}{\sqrt{\kappa^2+\eta^2}} & 0 \\ 0 & 1 & 0 & 0 \\ \frac{\eta}{\sqrt{\kappa^2+\eta^2}} & 0 & -\frac{\kappa}{\sqrt{\kappa^2+\eta^2}} & 0 \\ 0 & 0 & 0 & -1 \end{bmatrix} \tag{18}$$

After rotation of coordinates, the semiaxes for the ellipsoid are given by $\left(\sqrt{\frac{1-\sqrt{\kappa^2+\eta^2}}{1-\kappa^2-\eta^2}}, \sqrt{\frac{1+\sqrt{\kappa^2+\eta^2}}{1-\kappa^2-\eta^2}}, 1 \right)$.

Note the fact that any two of these values are not necessarily equal (for the general array orientation case) means that the ellipsoid is a triaxial ellipsoid.

A brief note on degenerate ellipsoids

In the case where Q is singular, we can have a so-called degenerate ellipsoid. One example, of several, is the ideal case where the array and the velocity vector are aligned in the horizontal plane (i.e., Figure 1a). For this specific case the matrix is obviously singular:

$$Q = \begin{bmatrix} 1 & -1 & 0 & 0 \\ -1 & 1 & 0 & 0 \\ 0 & 0 & 0 & 0 \\ 0 & 0 & 0 & 0 \end{bmatrix} \tag{19}$$

The important point about degenerate ellipsoids is that they still are a 3-dimensional surface even in the limit when one of the semiaxes goes to zero. One can think of this like a rugby ball that has the air removed to flatten it in one dimension. For our purpose this means that an intersection with a plane and a degenerate ellipsoid from equation (1) yields a line. Equation (19) results in a circle in 3-dimensions whose face is filled in. This provides more detail than the equation of the line as found in equation (3) for the 2-dimensional case.

6. ACKNOWLEDGMENTS

This work was partially funded under the Joint DoD/DOE Munitions Program Memorandum of Understanding.

Sandia National Laboratories is a multi-program laboratory managed and operated by Sandia Corporation, a wholly owned subsidiary of Lockheed Martin Corporation, for the U.S. Department of Energy's National Nuclear Security Administration under contract DE-AC04-94AL85000.

REFERENCES

[1] R. Klemm, *Principles of space-time adaptive processing*, IEE, (2002).
[2] P.G. Richardson, "Effects of manoeuvre on space time adaptive processing performance", Radar Conf 97, (1997).
[3] G. K. Borsari, "Mitigating effects on STAP processing caused by an inclined array", RADARCON 98, (1998).
[4] C. V. Jakowatz, Jr, D. E. Wahl, P. H. Eichel, D. C. Ghiglia, P. A. Thompson, *Spotlight-Mode Synthetic Aperture Radar: A Signal Processing Approach*, Kluwer Academic Publishers, (1996).